Rheological and Thermal Properties of Poly(ethylene oxide)/Multiwall Carbon Nanotube Composites

T. N. Abraham, Debdatta Ratna, S. Siengchin, J. Karger-Kocsis

Institute for Composite Materials, Technical University at Kaiserslautern, Erwin-Schrodinger-Straße 58, D-67663, Kaiserslautern, Germany

ABSTRACT: Poly(ethylene oxide) (PEO) based nanocomposites were prepared by the dispersion of multiwall carbon nanotubes (MWCNTs) in aqueous solution. MWCNTs were added up to 4 wt % of the PEO matrix. The dynamic viscoelastic behavior of the PEO/MWCNT nanocomposites was assessed with a strain-controlled parallel-plate rheometer. Prominent increases in the shear viscosity and storage modulus of the nanocomposites were found with increasing MWCNT content. Dynamic and isothermal differential scanning calorimetry studies indicated a significant decrease in the crystallization temperature as a result of the incorporation of MWCNTs; these composites can find applications as crystallizable switching components for shape-memory polymer systems with adjustable switching temperatures. The solid-state, direct-current conductivity was also enhanced by the incorporation of MWCNTs. The dispersion level of the MWCNTs was investigated with scanning electron microscopy. © 2008 Wiley Periodicals, Inc. J Appl Polym Sci 110: 2094–2101, 2008

Key words: differential scanning calorimetry (DSC); nanocomposites; rheology

INTRODUCTION

Nanocomposites are a new class of composites, which are particle-filled polymers for which at least one dimension of the dispersed particles is in the nanometer range. The extraordinary mechanical, electrical, and thermal properties of nanotubes make them outstanding materials to blend with polymers to prepare potentially multifunctional nanocomposites.[1,2] They offer novel properties because the distinct features of the inorganic and organic components[3,4] can be combined accordingly. The concept of nanoreinforcement is that the control of the structure/interactions at the smallest scale (i.e., the nanometer scale) provides the best option for tailoring the macroscopic properties of the related composites.[5] Among various available nanofillers, carbon nanotubes (CNTs) have been viewed as the most promising because of their attractive properties,[6] which include an exceptionally high aspect ratio (>300), a good elastic modulus (>1 TPa), and high thermal and electrical conductivities. This pseudo-one-dimensional form of carbon has remarkable physical and mechanical properties, such as structure-tunable electronic properties, ultrahigh thermal conductivity, and unmatched mechanical properties (e.g., stiffness, strength, resilience). These characteristics, combined with recent advances enabling the high-volume production of multiwall and single-wall nanotubes, offer tremendous opportunities for the development of ultra-high-performance nanotube-reinforced nanocomposite materials.[7]

The initial academic research on polymer/CNT nanocomposites has been focused on single-wall carbon nanotubes (SWCNTs) because of their simpler structure. However, the extremely high cost of SWCNTs considerably restricts the commercialization of CNT-based composites. That is why the technology of polymer/CNT nanocomposites is less mature compared to parallel contemporary issues, such as polymer/layered-silicate nanocomposites. However, the production of multiwall carbon nanotubes (MWCNTs) has already been scaled up by industry, and MWCNTs are available in sufficient quantities and at reasonable costs. Therefore, nowadays, research interest has been diverted toward the technological proliferation[8–10] of MWCNT-based systems. The uniform dispersion of MWCNTs within the polymer matrix and improved nanotube/matrix wetting and adhesion are critical issues with respect to the processing and application of these nanocomposites.[11,12]

Poly(ethylene oxide) (PEO) is a semicrystalline polymer, which has been considered in recent years for important applications, namely, biomedical[13] and electrochemical applications[14–16] and also as crystallizable switching segments for shape-memory polymer systems.[17–19] A common problem for all the

Correspondence to: D. Ratna, Naval Materials Research Laboratory, Additional Ambernath, Thane 421506, India (ratnad29@hotmail.com).

applications is linked with the poor mechanical properties of PEO. In addition, conventional PEO-based solid polymer electrolytes exhibit a low ionic conductivity, which is not sufficient for many applications. The incorporation of layered silicate is known to improve the mechanical properties and increase the conductivity of PEO-based electrolytes, as the silicate layers act as anions, and hence, the cation can preferentially move.[20,21] However, even such modification cannot raise the conductivity high enough to meet the demand. MWCNTs, being inherently conducting, may be a better candidate for the modification of PEO-based electrolytes. In case of shape-memory polymers, the incorporation of MWCNTs, in addition to their reinforcing effect, is expected to offer electrically induced actuation, which can be controlled remotely (via Joule heating).[21] Therefore, our work should also shed light on specific approaches for the creation of PEO nanocomposites with improved mechanical properties.

Recently, researchers have reported the enhancement of the rheological properties of PEO with the addition of MWCNTs.[22,23] However, a detailed investigation of the crystallization behavior of the nanocomposite is required to design a PEO-based crystallizable component for shape-memory polymer systems with adjustable switching temperatures.[24] This study focused on the preparation, characterization, crystallization, and rheological behavior of PEO/MWCNT nanocomposites.

EXPERIMENTAL

Materials

The matrix PEO, with a weight-average molecular weight of 300,000 g/mol, was purchased from Acros Organics (Geel, Belgium). MWCNTs (Baytube 150P) were procured from Bayer Material Science AG (Leverkusen, Germany). The MWCNTs had a purity greater than 95%, outer diameters within the range 13–16 nm, and an average length between 1 and 10 μm (data provided by the manufacturer). Distilled water was used as a solvent.

Preparation of the PEO/MWCNT nanocomposites

Nanocomposite films were made by the dispersion of MWCNTs in an aqueous solution of PEO (5 wt %) with the sonication method using a mechanical probe sonicator (19 mm diameter, maximum power 1000 W, frequency 20 kHz; Branson ultrasound PGB210A, Danbury, CT). The required amount of MWCNTs was accurately weighed and placed in a beaker. Double-distilled water (250 mL) was added, and the whole mixture was sonicated for 15 min. The aqueous PEO solution (the required amount of PEO dissolved in water) was added to the same beaker. The mixture was again sonicated for 20 min, and the mixture was poured in aluminum molds and kept in an air-ventilated oven at 50°C for 2 days. During the whole process of sonication, the beaker was immersed in cold water. The films were then dried *in vacuo* at 50°C for 24 h at 10^{-2} bar of pressure. The PEO/MWCNT nanocomposites were designated as PEO/MWCNT (0.4 wt %), PEO/MWCNT (1 wt %), PEO/MWCNT (2 wt %), and PEO/MWCNT (4 wt %), depending on the concentration of MWCNTs.

Characterization

Differential scanning calorimetry (DSC)

The thermal behavior of the PEO and the PEO/MWCNTs was studied with a differential scanning calorimeter (Mettler–Toledo DSC821, Greifensee, Switzerland). All of the samples were dried before the measurements, and the analyses were carried out in a nitrogen atmosphere with standard aluminum pans. About 10 mg of sample was placed in an aluminum pan and heated from 25 to 90°C at a heating rate of 10°C/min. The melted sample was then cooled to 25°C at a cooling rate of 10°C/min. The samples were subsequently reheated to 90°C at a rate of 20°C/min, held at 90°C for 2 min, and then cooled rapidly (60°C/min) to the desired temperature (35, 40, or 45°C) for the isothermal crystallization studies. To study the effect of the cooling rate on crystallization, the pure PEO sample was cooled at different cooling rates, including 1, 3, 5, 15, 20,and 25°C/min.

We calculated the melting point, crystallization temperature (T_c), and enthalpy of crystallization (ΔH_c) from the DSC curves considering the maximum position of the endothermic/exothermic peaks and the area of crystallization curve under the DSC thermograms, respectively.

Scanning electron microscopy (SEM)

The morphology of the PEO and PEO/MWCNTs was investigated by a high-resolution Zeiss Supra 40 VP scanning electron microscope (Carl Zeiss SMT, Oberkochen, Germany). Compression-molded samples were quenched in liquid nitrogen and cryogenically fractured. The fracture surfaces were sputter-coated with carbon before SEM observation to avoid charging.

Viscoelastic measurements

Viscoelastic properties of the PEO/MWCNTs were studied with a strain-controlled rheometer (ARES of Rheometric Scientific, Piscataway, NJ) equipped
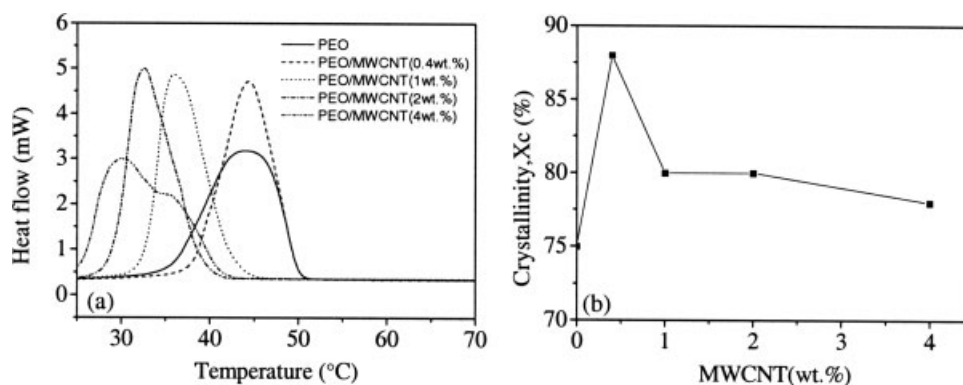
Figure 1 DSC crystallization plots of the PEO/MWCNT nanocomposite: (a) the effect of T_c with the MWCNT concentration and (b) the effect of X_c with the MWCNT concentration.

with stainless steel parallel disks 25 mm in diameter. Measurements were performed with the oscillatory shear method at different temperatures. Test specimens were prepared by compression molding of the solution-cast film at 100°C for about 5 min to for disks 2 mm thick and 25 mm in diameter. In the linear viscoelastic measurements, the dynamic strain sweep measurements were carried out first to determine the linear region (<3% change in the storage modulus). In the oscillatory shear experiments, a sinusoidal shear strain, $\gamma(t) = \gamma_0 \sin(\omega t + \phi)$, where ω is the angular frequency, γ_0 is the constant oscillatory strain, and t is the time, was imposed. In the frequency sweep measurements, γ_0, the frequency-dependent elastic modulus (G'), and the complex viscosity (η^*) were determined.

Conductivity measurements

The solid-state, direct-current electrical conductivity was measured with the magnetic carpet probe method with a highly precise resistivity meter (Hiresta-UP, MCP-HT450, Mitsubishi Chemical, Kanagawa, Japan). Depending on the probe selected, the correction factors were automatically set, and the resistance value could be directly obtained from the measuring device.

RESULTS AND DISCUSSION

Crystallization behavior

It is well known that the crystallization behavior of a semicrystalline polymer is affected by the presence of any fillers and depends on two factors: (1) the entropic contribution to the free energy of formation of a nucleus of critical dimension that represents the probability of selecting the required number of crystallite sequences from the mixture and (2) the energy required for the transport of the other component from the growth front into the interlaminar region.[25,26]

We studied the crystallization behavior of the PEO/MWCNT nanocomposites with DSC, as disclosed in the Experimental section. The effect of MWCNT content on the crystallization peak of the nanocomposite is shown in Figure 1. From the crystallization plots, the specific heat of crystallization of the nanocomposite (ΔH_c^{comp}) was calculated with the following formula:

$$\Delta H_c^{\text{comp}} = \frac{(\Delta H_c)_{\text{total}} \times 100}{x \times z} \tag{1}$$

where $(\Delta H_c)_{\text{total}}$ is obtained from the peak area of the DSC cooling curve, x is the weight of the sample taken for the DSC experiment, and z is the concentration of PEO (wt %). The degree of crystallinity (X_c) of the nanocomposites was calculated from the following formula:

$$X_c = \Delta H_c^{\text{comp}} / \Delta H_c^0 \tag{2}$$

where ΔH_c^0 is the specific heat of crystallization of 100% crystalline PEO (205 J/g).[27]

As shown in Figure 1(a), it was evident that the T_c for the PEO/MWCNT nanocomposites at lower MWCNT concentrations remained the same as that of PEO but decreased with increasing loading of the MWCNTs. Although T_c decreased, X_c was not affected much compared with that of the PEO matrix. At lower concentrations of MWCNTs, X_c was enhanced in the PEO/MWCNT nanocomposites [Fig. 1(b)]. Clearly, detailed studies need to be conducted to fully understand the effect of the addition of MWCNTs on the crystalline morphology and crystallization mechanism. The unique character of PEO, which exhibits crystallization enhancement in the presence of inorganic fillers but at the same time has its crystallization hindered by the addition of alkali cations, was reported earlier.[28–30] From the
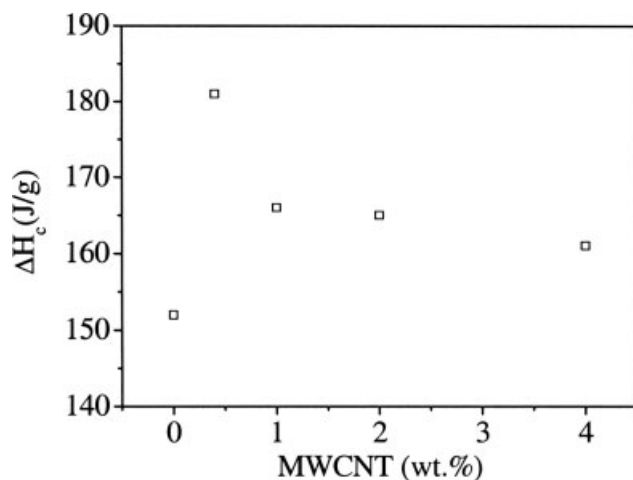
Figure 2 Variation in ΔH_c of the PEO/MWCNT nanocomposites with the MWCNT concentration.

previously mentioned crystallization plot [Fig. 1(a)], ΔH_c values of the PEO/MWCNT nanocomposites were calculated and are plotted in Figure 2. The ΔH_c values of the PEO/MWCNT nanocomposite were also found to increase compared to those of PEO. Krishnamoorti et al.[31] investigated the crystallization kinetics of PEO-based nanocomposites in which SWCNTs were dispersed with surfactants and reported that the crystallization process was disturbed (T_c decreased) and demonstrated a decrease in crystallinity. The effects of the cooling rate on T_c for PEO, PEO/MWCNT (2 wt %), and PEO/MWCNT (4 wt %) are shown in Figure 3. As expected, T_c decreased with increasing cooling rate, but the reduction was more prominent the nanocomposite with higher MWCNT concentration, especially at a higher cooling rates than that of the neat PEO.
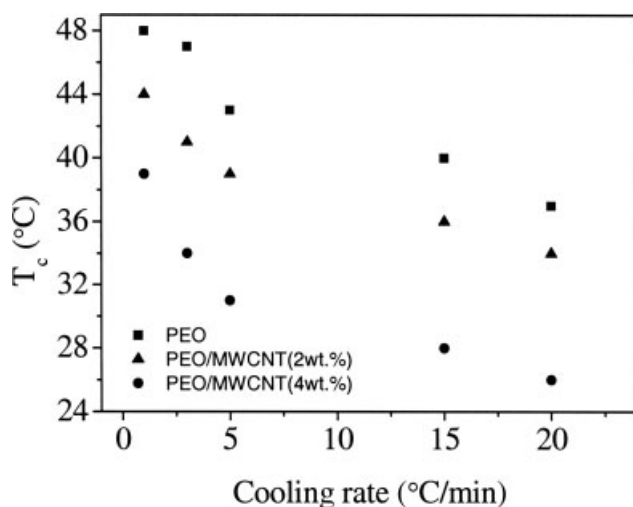
From the dynamic crystallization studies, it was evident that the T_c of the nanocomposites gradually decreased with increasing MWCNT concentration. To gather detailed knowledge of the rate of crystallization, we carried out isothermal crystallization studies for PEO and PEO/MWCNT (4 wt %). Figure 4 shows the typical isothermal crystallization curves at three different temperatures (35, 40, and 45°C). The time corresponding to the maximum heat flow rate (exotherm) was taken as the peak time of crystallization (t_{peak}). PEO showed t_{peak} at 70, 96, and 106 s at isothermal T_c values of 35, 40, and 45°C, respectively. PEO/MWCNT (4 wt %) displayed peaks like PEO at isothermal T_c values of 35°C (t_{peak} = 76 s) and 40°C (t_{peak} = 120 s) with delayed or lower crystallization. The crystallization was so slow that no complete crystallization peak was displayed when T_c was set at 45°C. As also shown in Figure 4, the t_{peak} value for the nanocomposite was higher than that of the PEO alone.

Both the dynamic and isothermal DSC experiments clearly indicated that the rate of crystallization decreased because of the addition of MWCNTs.
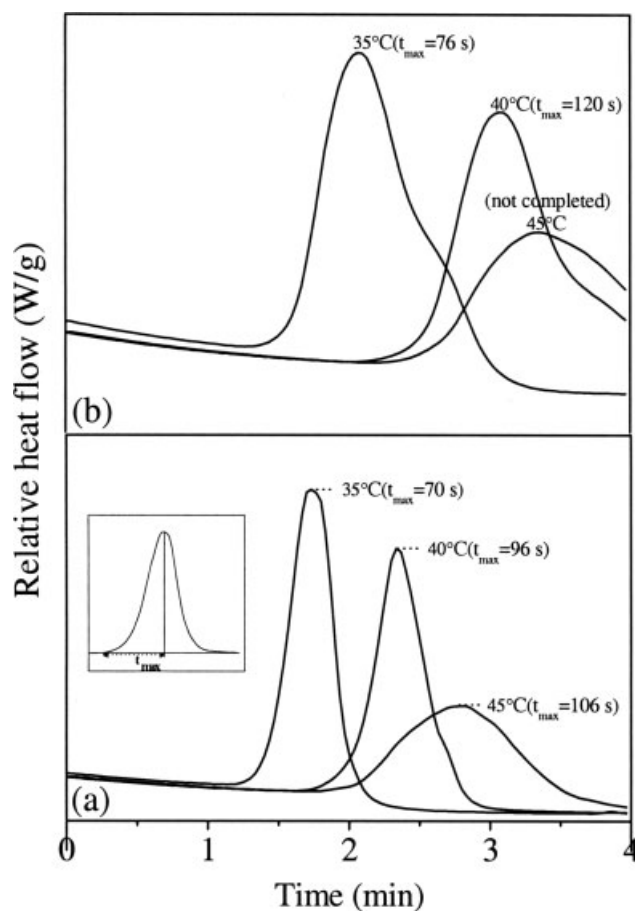

Figure 3 Effect of the cooling rate on T_c of the PEO/MWCNT nanocomposite.

Figure 4 Heat flow during the isothermal crystallization of the PEO/MWCNT nanocomposite: (a) PEO and (b) PEO/MWCNT (4 wt %). t_{max} is the maximum time.
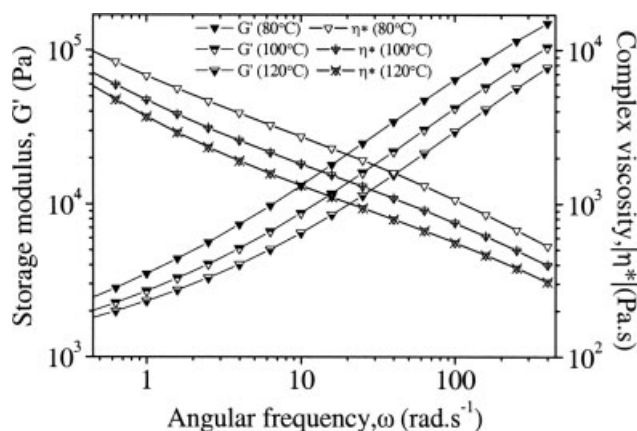
Figure 5 Variation of G' and η^* versus the shear rate for PEO/MWCNT (2 wt %) at 80, 100, and 120°C.

It is interesting to note that with the addition of 2 wt % MWCNTs, it was possible to change T_c from 45 to 30°C, whereas about 80% crystallinity was retained [Fig. 1(b)]. Thus, it was possible to change the transition temperature without appreciably affecting the crystallinity. Because PEO is used as a crystallizable switching segment, the switching temperature can be adjusted on request for various applications, such as for biomedical use (~35°C).

Rheological measurements of the PEO and PEO/MWCNTs were carried out with a parallel-plate rheometer, as disclosed in the Experimental section, at three different temperatures (80, 100, and 120°C) and a frequency range of 0.1–398 rad/s. The nanocomposite showed typical pseudoplastic behavior, and the viscosity decreased with temperature as expected [shown in Fig. 5 for PEO/MWCNT (2 wt %)]. The effect of the temperature on the shear viscosity is generally explained by the fact that an increase in temperature leads to intense thermal motion of the molecules and generates a larger free volume in the polymer accompanied with a decrease in the intermolecular or intramolecular association.[32,33] The

storage modulus of the nanocomposites also diminished with increasing temperature, which means that the material had a lower relaxation time when the temperature increased.[33]

The shear viscosity of the pure polymer was characterized by two distinct regions, called the *Newtonian* and *shear thinning regions*. At low shear rate, the Newtonian region with independence of shear rate was observed, followed by the shear thinning region, where the viscosity linearly decreased with an increase in the shear rate. We compare the viscosity of various compositions at 80°C in Figure 6(a). The nanocomposites displayed considerably higher viscosity and dynamic storage modulus values than the PEO matrix over all of the shear rates investigated, especially at lower shear rates. As shown in Figure 6(a), as the MWCNT loading increased in the nanocomposites, the Newtonian region disappeared, and only the shear thinning region remained throughout the entire shear rate range. When the MWCNT concentration was higher than 1 wt %, the Newtonian plateau region completely shifted to the shear thinning region. This was supported by the power-law index values obtained for the PEO/MWCNTs, as shown in Table I. The flow behavior index values of the nanocomposites were higher than that of PEO matrix up to 1 wt % MWCNTs and, thereafter, decreased. In general, the viscosity increased in the nanocomposites because of two types of interactions, namely, particle–polymer interaction and particle–particle interaction. The particle–particle interactions, which resulted in an increase in the shear viscosity without the Newtonian plateau region, played a dominant role in the rheological behavior of the nanocomposites. The pronounced increase in the viscosity of the polymer composites with MWCNTs (or any other anisotropic filler such as layered silicate) is often attributed to the formation of a hydrodynamically percolated filler network structure and usually correlated with the level of
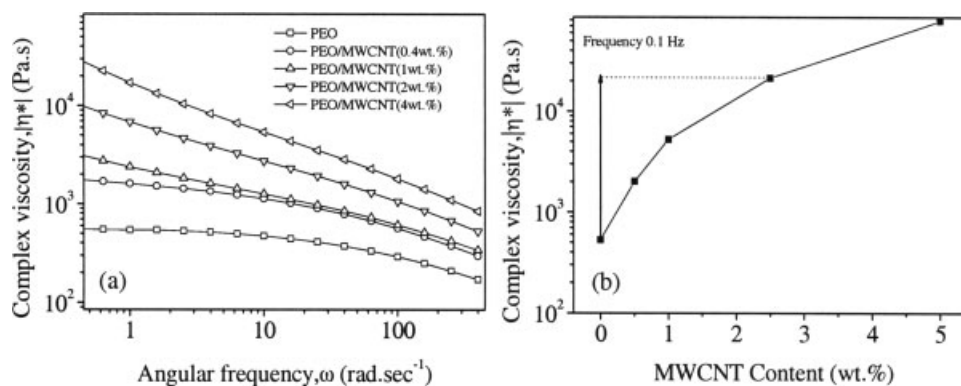

Figure 6 η^* measurements at 80°C: (a) ω dependence of η^* for the PEO/MWCNT nanocomposite with various concentrations of MWCNTs and (b) η^* of the PEO/MWCNT nanocomposite at 0.1 Hz as a function of the MWCNT concentration.

TABLE I
Power-Law Index and Activation Energy of PEO and
PEO/MWCNT

Sample	Flow behavior index at 80°C	Activation energy (kJ/mol)	
		398 rad/s	0.1 rad/s
PEO	0.646	5.9	9.2
PEO/MWCNT (0.4 wt %)	0.768	8.5	12.9
PEO/MWCNT (1 wt %)	0.676	7.5	5.1
PEO/MWCNT (2 wt %)	0.558	6.7	3.8
PEO/MWCNT (4 wt %)	0.450	6	2.2

dispersion of the filler.[34,35] The plots of η^* at 0.1 rad/s as a function of MWCNT concentration are also shown in Figure 6(b). The plots clearly indicate the rheological percolation of about 1 wt % of MWCNTs. The very low percolation of the MWCNTs arose because of their high aspect ratio. Note that 30 vol % isotropic spheres was required for the percolation in three dimensions.[36,37] However, it was much higher than the theoretical percolation threshold value, which indicated that that the MWCNTs were not fully exfoliated.

The enhancement in viscosity could also be explained in terms of the confinement of polymer chains within the nanotube layer.[38,39] The viscosity of the confined polymer melt is always greater than that of the bulk. The higher viscosity of the confined melt is believed to arise from an immobilized hydrodynamic layer near the wall with a thickness on the order of the radius of gyration of the polymer chain. According to Subbotin et al.,[38] for the shear flow of melts confined between parallel plates separated by a distance $h/a \sim N^{1/2}$, where a is the segment length and N is the number of segments in the polymer chain, the relative zero-shear viscosity of the confined melt (η_0^c) with respect to the bulk viscosity (η_0^b) can be determined as follows:

$$\frac{\eta_0^c}{\eta_0^b} \approx \frac{a}{h}\frac{\lambda^c}{\lambda^b} \approx \left(\frac{h}{a}\right)^2 \text{ for } \lambda^c/\lambda^b \approx (h/a)^3 \quad (3)$$

where λ^c and λ^b are the segment relaxation times of the confined and bulk polymer chains, respectively. Thus, the scaling model predicts that $\lambda^c \gg \lambda^b$, and if the separation distance were on the order of the radius of gyration of the polymer chain, the zero-shear viscosity of the confined system would scale as N, which is about 50–100 in case of PEO. Hence, the viscosity of the PEO/MWCNT melt was several times higher than that of the bulk melt, as reflected in our viscosity data from low shear rate. Song[40] reported an increase in the viscosity with the addition of acid-treated MWCNTs in the PEO matrix and

demonstrated a higher effective volume fraction of MWCNTs than of the real one.

Figure 7 shows the linear dynamic oscillatory frequency dependence of G' as a function of MWCNT loading for the prepared PEO nanocomposites. The pure polymer behaves like a Newtonian liquid with characteristic low-frequency terminal behavior ($G' \alpha \omega^\beta$, $\beta = 2.0$). The incorporation of MWCNTs into this polymer resulted in an increase in G' at all frequencies and a decreased low-frequency power-law scaling of G' (β values, shown in the inset of Fig. 7). This suggested that stress relaxation was effectively arrested by the presence of the MWCNTs. G' was almost independent of ω at low frequencies; at a low concentration of MWCNTs, this was indicative of a transition from liquidlike to solidlike viscoelastic behavior. At high oscillation frequencies, the effect of particle loading was relatively weak. This result suggested that the influence of the MWCNTs on the stress relaxation dynamics was much stronger than their influence on the plateau elastic modulus. Zhang and Archer[41] reported a similar behavior of transition at a particle volume fraction of 2% for PEO/silica nanocomposites.

We measured the dynamic rheological behaviors of the PEO and PEO/MWCNTs at various temperatures and calculated the flow activation energy with the following Arrhenius equation:[42,43]

$$\eta_\gamma = A \exp\left(\frac{E_\gamma}{RT}\right) \quad (4)$$

where η_γ and E_γ are the apparent viscosity and activation energy, respectively, at a given shear rate; A is a constant; R is the gas constant; and T is the absolute temperature.
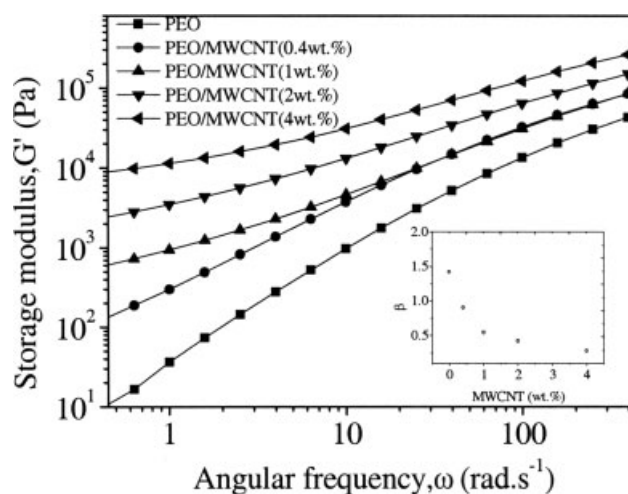

Figure 7 Variation of G' with the MWCNT concentration. The inset shows the low-frequency power-law scaling (β) of G'. The rheological measurements were performed at 80°C.
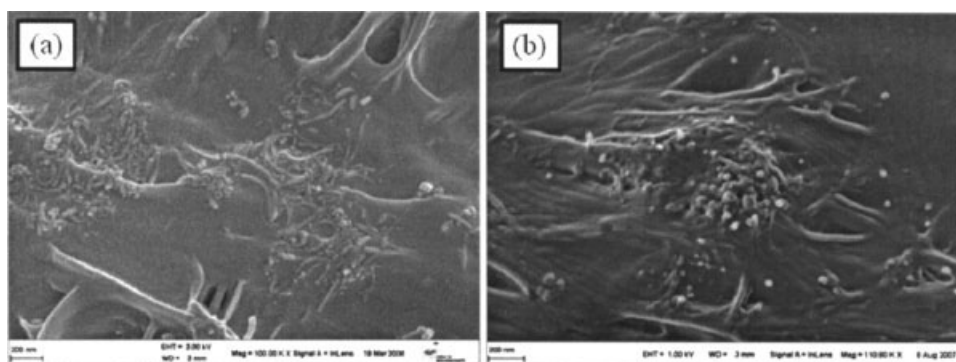
Figure 8 SEM microphotographs of cryofractured samples of (a) PEO/MWCNT (0.4 wt %) and (b) PEO/MWCNT (2 wt %).

Thus, E_γ at a given shear rate could be obtained directly from plots of ln η_γ against $1/T$. The calculated activation energies at different shear rates for the PEO/MWCNTs are shown in Table I. The computed activation energies decreased with increasing shear rate. According to certain established molecular theories for viscous flow, the activation energy may be taken as a measure of the potential energy barrier that is associated with movement of the molecules.[44,45] Under the action of a shear stress, the alignment, orientation, and disentanglement of a polymer chain occur, and this enables the polymer molecules to move more easily. This, in turn, is accompanied with a corresponding decrease in the activation energy with increasing shear rate. It was also observed that the activation energy of PEO increased with the addition of MWCNTs, as shown in Table I. The enhancement of the activation energy of the nanocomposites could be explained well by the high aspect ratio and surface area of the MWCNTs, which created the formation of the percolation structure, which in turn, increased the particle–polymer interactions. This filler network more easily made strong particle–polymer interactions at low filler concentrations because the interfacial area between the particles and polymer dramatically increased. Therefore, the activation energy for PEO/MWCNTs at lower concentration was higher than at higher concentrations of MWCNTs.

The particle–polymer interactions could be explained by the level of dispersion of the MWCNTs in the PEO matrix, as analyzed by SEM. The SEM photographs of PEO/MWCNT (0.4 wt %) and PEO/MWCNT (2 wt %) are shown in Figure 8. It is evident from the figure that, at lower concentrations, the nanotubes were well dispersed in the matrix, whereas at higher concentrations, a lot of agglomerates could be seen, which reduced the particle–polymer interactions. The result was consistent with that observed in case of polypropylene-based clay/nanocomposites, where no change[35] or increase[46] in activation energy was reported.

The solid-state, direct-current conductivity measurements at room temperature showed that the conductivity increased monotonically with increasing nanotube concentration, and this trend followed other reports of electrical conductivity in polymer–nanotube composites.[47,48] Figure 9 indicates an electrical percolation of less than 1 wt % MWCNT concentration, which was consistent with the percolated network structure observed in the rheological measurements, as discussed earlier. The modification of MWCNT to improve the dispersion and decrease the percolation threshold further is in progress and will be presented in a later communication.
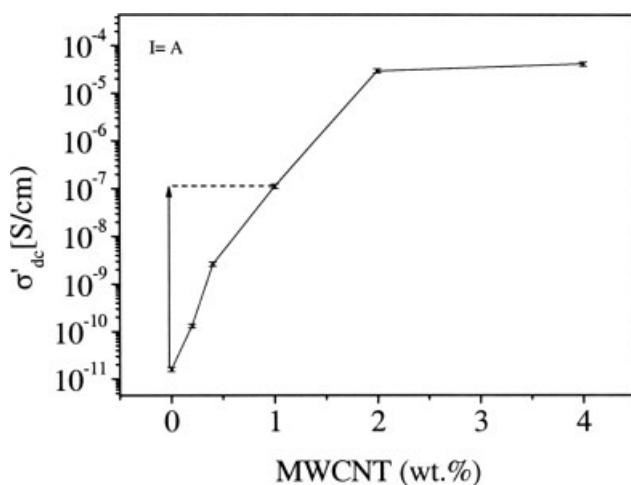

Figure 9 Solid-state direct-current conductivity (σ'_{dc}) measurements for PEO/MWCNT versus the MWCNT concentration at room temperature.

CONCLUSIONS

We created PEO–MWCNT nanocomposites by dispersing MWCNTs in an aqueous PEO solution with the help of a sonicator. Dynamic viscoelastic measurements demonstrated a significant increase in the viscosity (at all of the shears rate used) with the addition of the MWCNTs. As expected, the melts were pseudoplastic in nature, and the viscosity decreased with

increasing temperature. Both the rheological and conductivity studies showed that there existed electrical percolation at about 1 wt % MWCNTs in the PEO nanocomposites. Dynamic and isothermal DSC crystallization studies showed a considerable decrease in the rate of crystallization without much effect on the overall crystallinity. Thus, T_c could be reduced and manipulated by a change in the MWCNT concentration. This indicated the suitability of the PEO-based nanocomposites for use as crystallizable switching components (with adjustable switching temperatures) for shape-memory polymer systems. Detailed studies on the crystallization mechanism of PEO upon incorporation of MWCNTs are currently underway.

References

1. Ajayan, P. M. Chem Rev 1999, 99, 1787.
2. Saito, R.; Dresselhaus, G.; Dresselhaus, M. S. Physical Properties of Carbon Nanotubes; Imperial College: London, 1998.
3. Schaefer, W. D.; Justice, S. R. Macromolecules 2007, 40, 8501.
4. Sanchez, C.; Julián, B.; Belleville, P.; Popall, M. Mater Chem 2005, 15, 3559.
5. Wang, M. J. Rubber Chem Technol 1998, 71, 520.
6. Treacy, M. M. J.; Ebbesen, T. W.; Gibson, J. M. Nature 1996, 381, 678.
7. Thostenson, E. T.; Ren, Z. F.; Chou, T. W. Compos Sci Technol 2001, 61, 1899.
8. Kong, H.; Gao, C.; Yan, D. Macromolecules 2004, 37, 4022.
9. Hong, C.-Y.; You, Y.-Z.; Pan, C.-Y. J Polym Sci Part A: Polym Chem 2006, 44, 2419.
10. Du, J. H.; Bai, J.; Cheng, H. M. Express Polym Lett 2007, 1, 253.
11. Andrews, R.; Weisenberger, M. C. Curr Opin Solid State Mater Sci 2004, 8, 31.
12. Lin, Y.; Meziani, M. J.; Sun, Y.-P. J Mater Chem 2007, 17, 1143.
13. Alcantar, N. A.; Aydil, E. S.; Israelachvili, J. N. J Biomed Mater Res 2000, 51, 343.
14. Yang, X. Q.; Hanson, L.; McBreen, J.; Okamoto, Y. J Power Sources 1995, 54, 198.
15. Mishra, R.; Rao, K. J. Solid State Ionics 1998, 106, 113.
16. Aranda, P.; Mosqueda, Y.; Perez-Cappe, E.; Ruiz-Hitzky, E. J Polym Sci Part B: Polym Phys 2003, 41, 3249.
17. Kuo, S. W.; Lin, C. L.; Chang, F. C. Macromolecules 2002, 35, 278.
18. Talibuddin, S.; Wu, L.; Runt, J.; Lin, J. S. Macromolecules 1996, 29, 7527.
19. Ratna, D.; Divekar, S.; Samui, A. B.; Chakraborty, B. C.; Banthia, A. K. Polymer 2006, 47, 4068.
20. Ratna, D.; Divekar, S.; Sivaraman, P.; Samui, A. B.; Chakraborty, B. C. Polym Int 2007, 56, 900.
21. Vaia, R. Nat Mater 2005, 4, 429.
22. Song, Y. S. Polym Eng Sci 2006, 46, 1350.
23. Shieh, Y.-T.; Liu, G.-L.; Hwang, K. C.; Chen, C.-C. Polymer 2006, 49, 10945.
24. Ratna, D.; Karger Kocsis, J. J Mater Sci 2007, 43, 254.
25. Martuscelli, E. Polym Eng Sci 1984, 24, 563.
26. Alfanso, G. C.; Russel, T. P. Macromolecules 1986, 19, 1143.
27. Chen, H. W.; Chang, F. C. Polymer 2001, 42, 9763.
28. Gadjourova, Z.; Andreev, Y. G.; Tunstall, D. P.; Bruce, P. G. Nature 2001, 412, 520.
29. Edman, L.; Ferry, A.; Doeff, M. M. J Mater Res 200, 15, 1950.
30. Strawhecker, K. E.; Manias, E. Chem Mater 2003, 15, 844.
31. Chatterjee, T.; Yurekli, K.; Hadjiev, V. G.; Krishnamoorti, R. Adv Funct Mater 2005, 15, 1832.
32. Choi, H. J.; Kim, S. G.; Hyun, Y. H.; Jhon, M. S. Macromol Rapid Commun 2001, 22, 320.
33. Cai, A. H.; Ailt-Kadi; Brisson, J. Polymer 2003, 44, 1481.
34. Wu, D.; Wu, L.; Zhang, M. J Polym Sci Part B: Polym Phys 2007, 45, 2239.
35. Galgali, G.; Ramesh, C.; Lele, A. Macromolecules 2001, 34, 852.
36. Mitchell, C. A.; Bahr, J. L.; Arepalli, A.; Tour, J. M.; Krishnamoorti, R. Macromolcules 2002, 35, 8825.
37. Garboczi, E. J.; Snyder, K. A.; Douglas, J. F.; Thorpe, M. F. Phys Rev E 1995, 52, 819.
38. Subbotin, A.; Semenov, A.; Doi, M. Phys Rev E 1997, 56, 623.
39. Khare, R.; Pablo, J.; Yethiraj, A. M. Macromolecules 1996, 29, 7910.
40. Song, Y. S. e-Polymers 2007, No. 047.
41. Zhang, Q.; Archer, A. L. Langmuir 2002, 18, 10435.
42. Nielson, L. Polymer Rheology; Marcel Dekker: New York, 1997.
43. Xiong, Y.; Kiran, E. Polymer 1997, 38, 4817.
44. Vaia, R. A.; Vasudevan, S.; Krawiec, W.; Scunlon, L. G.; Giannelis, E. P. Adv Mater 1995, 7, 2.
45. Cogswell, F.; McGowan, J. Br Polym J 1972, 4, 183.
46. Gu, S.-Y.; Ren, J.; Wang, Q.-F. J Appl Polym Sci 2004, 91, 2427.
47. Du, F. M.; Fischer, J. E.; Winey, K. I. J Polym Sci Part B: Polym Phys 2003, 41, 3333.
48. Ramasubramaniam, R.; Chen, J.; Liu, H. Y. Appl Phys Lett 2003, 83, 2928.